

Phase separation and pattern instability of laser-induced polymerization in liquid-crystal-monomer mixtures

Chandroth P. Jisha,^{1,2} Kuei-Chu Hsu,³ YuanYao Lin,^{1,2} Ja-Hon Lin,⁴
Kai-Ping Chuang,⁵ Chao-Yi Tai,⁶ and Ray-Kuang Lee^{1,2,*}

¹*Institute of Photonics Technologies, National Tsing-Hua University, Hsinchu 300, Taiwan*

²*Frontier Research Center on Fundamental and Applied Sciences of Matters,
National Tsing-Hua University, Hsinchu 300, Taiwan*

³*Unice E-O Services Inc., Chungli 320, Taiwan*

⁴*Department of Electro-Optical Engineering and Institute of Electro-Optical Engineering,
National Taipei University of Technology, Taipei 106, Taiwan*

⁵*Center for Measurement Standards, Industrial Technology Research Institute, Hsinchu 300,
Taiwan*

⁶*Department of Optics and Photonics, National Central University, Chung-Li 320, Taiwan*

[*rkleee@ee.nthu.edu.tw](mailto:rkleee@ee.nthu.edu.tw)

Abstract: Directly written by a ultra-short femto-second laser pulse, we report the phase separation and pattern formation induced by polymerization in a liquid-crystal-monomer mixture. By varying the scanning speed of optical fields along a line, pattern transitions of photon-induced polymer structures are illustrated in shapes of double-humped, single-humped, and broken stripes. The experimental data collected by optical microscopic images are in a good agreement with numerical simulations based on a modified set of coupled $2 + 1$ dimensional diffusion equations. The demonstration in this work provides a step for controlling phase separation morphologies as well as transferring patterns in polymer-dispersed liquid crystals.

© 2011 Optical Society of America

OCIS codes: (160.3710) Liquid crystals; (140.3390) Laser materials processing; (230.3720) Liquid-crystal devices; (190.4420) Nonlinear optics, transverse effects in; (190.4710) Optical nonlinearities in organic materials.

References and links

1. D. K. Yang and S. T. Wu, *Fundamental of Liquid Crystal Devices* (Wiley, 2006).
2. S. Moynihan, P. Lovera, D. O'Carroll, D. Iacopino, and G. Redmond, "Alignment and dynamic manipulation of conjugated polymer nanowires in nematic crystal hosts," *Adv. Mater.* **20**, 2497–2502 (2008).
3. H. Tanaka, "Formation of network and cellular structures by viscoelastic phase separation," *Adv. Mater.* **21**, 1872–1880 (2009).
4. H. Kikuchi, M. Yokota, Y. Hisakado, H. Yang, and T. Kajiyama, "Polymer-stabilized liquid crystal blue phases," *Nat. Mater.* **1**, 64–68 (2002).
5. S.-Y. Lu and L.-C. Chien, "Electrically switched color with polymer-stabilized blue-phase liquid crystals," *Opt. Lett.* **35**, 562–564 (2010).
6. J. Y. Kim, C. H. Cho, P. Palfy-Muhoray, M. Mustafa, and T. Kyu, "Polymerization-induced phase separation in a liquid-crystal-polymer mixture," *Phys. Rev. Lett.* **71**, 2232–2235 (1993).
7. J. Y. Kim, H. Y. Woo, J. W. Baek, T. W. Kim, E. A. Song, S. C. Park, and D. W. Ihm, "Polymer-dispersed liquid crystal devices using highly conducting polymers as electrodes," *Appl. Phys. Lett.* **92**, 183301 (2008).
8. H. Ren, S. T. Wu, and Y. H. Lin, "In situ observation of fringing-field-induced phase separation in a liquid-crystal-monomer mixture," *Phys. Rev. Lett.* **100**, 117801 (2008).

9. E. A. Buyuktanir, M. W. Frey, and J. L. West, "Self-assembled, optically responsive nematic liquid crystal/polymer core-shell fibers: Formation and characterization," *Polymer* **51**, 4823–4830 (2010).
10. R. Sigel, G. Fytas, N. Vainos, S. Pispas, and N. Hadjichristidis, "Pattern formation in homogeneous polymer solutions induced by a continuous-wave visible laser," *Science* **297**, 67–69 (2000).
11. S. Matsuo, S. Juodkazis, and H. Misawa, "Femtosecond laser microfabrication of periodic structures using a microlens array," *Phys. Rev. A* **80**, 683–685 (2005).
12. Y. Ichihashi, P. Henzi, M. Bruendel, J. Mohr, and D. G. Rabus, "Polymer waveguides from alicyclic methacrylate copolymer fabricated by deep-UV exposure," *Opt. Lett.* **32**, 379–381 (2007).
13. C. H. Lee, H. Yoshida, Y. Miura, A. Fujii, and M. Ozaki, "Local liquid crystal alignment on patterned micro-grating structures photofabricated by two photon excitation direct laser writing," *Appl. Phys. Lett.* **93**, 173509 (2008).
14. K. Tokuoka, H. Yoshida, Y. Miyake, C. H. Lee, Y. Miura, S. Yusuke, F. Satoshi, A. Fujii, Y. Shimizu, M. Ozaki, "Planar alignment of columnar liquid crystals in microgroove structures," *Mol. Cryst. Liq. Cryst.* **510**, 126–133 (2009).
15. Data Sheet Licristal®E7, (Merck KGaA, Germany, 2001).
16. N. Gheorghiu, J. L. West, A. V. Glushchenko, and M. Mitrokhin, "Patterned field induced polymer walls for smectic A bistable flexible displays," *App. Phys. Lett.* **88**, 263511 (2006).
17. Yu. S. Kivshar and D. E. Pelinovsky, "Self-focusing and transverse instabilities of solitary waves," *Phys. Rep.* **331**, 117–195 (2000).
18. Y. Y. Lin, R.-K. Lee, and Yu. S. Kivshar, "Soliton transverse instabilities in nonlocal nonlinear media," *J. Opt. Soc. Am. B* **25**, 576–581 (2008).
19. Y. Y. Lin, R.-K. Lee, and Yu. S. Kivshar, "Transverse instability of TM solitons and nonlinear surface plasmons," *Opt. Lett.* **34**, 2982–2984 (2009).
20. C. C. Bowley and G. P. Crawford, "Diffusion kinetics of formation of holographic polymer-dispersed liquid crystal display materials," *Appl. Phys. Lett.* **76**, 2235–2237 (2000).
21. P. Rathi and T. Kyu, "Theory and computation of photopolymerization-induced phase transition and morphology development in blends of crystalline polymer and photoreactive monomer," *Phys. Rev. E* **79**, 031802 (2009).
22. Q. Wang, D. Zhang, Y. Huang, Z. Ni, J. Chen, Y. Zhong, and S. Zhuang, "Type of tunable guided-mode resonance filter based on electro-optic characteristic of polymer-dispersed liquid crystal," *Opt. Lett.* **35**, 1236–1238 (2010).
23. P. G. D. Gennes and J. Prost, *The Physics of Liquid Crystals* (Oxford University Press, 1995).
24. S. R. Challa, S.-Q. Wang, and J. L. Koenig, "In situ diffusion studies using spatially resolved infrared microspectroscopy," *Appl. Spectrosc.* **50**, 1339–1344 (1996).
25. C.-C. Jeng, Y. Y. Lin, R.-C. Hong, and R.-K. Lee, "Optical pattern transitions from modulation to transverse instabilities in photorefractive crystals," *Phys. Rev. Lett.* **102**, 253905 (2009).

With electrical and optical tunabilities, polymer-dispersed liquid crystals (PDLCs), composited by spreading sub-micron sized liquid crystal (LC) droplets in a polymer matrix, have shown a variety of applications in optical devices from light switches, phase modulators, holographic gratings, to flat panel displays [1]. Even though low-molecular-weight liquid crystal droplets and high-molecular-weight polymers together form a heterogeneous system, possible phase separations in a PDLC system have been demonstrated due to the reduction of mixing entropy in the polymerization process. Spontaneous phase separations have been used to generate anisotropic nano-structures and to monitor pattern evolutions in both soft and hard matters [2,3]. Especially, nowadays the polymer-stabilized blue-phase mode is intensively employed in liquid crystal displays and photonic devices for its unique electro-optic performances [4,5].

It is known that polymerization processes can be induced and controlled by curing temperature, ultraviolet (UV) light exposure intensities, material concentrations, or fringing electric-fields [6–9]. Among thermal, photo, solvent, and electrical approaches, UV light exposures have been widely adopted to induce polymerization in micro- and nano-machining, due to their feasibility in optical lithography technologies [10–14]. In contrast to a random droplet distribution in the conventional PDLCs, the approach of direct laser writing provides an alternative method to manipulate spatial distribution of liquid crystals within. Although the kinetics of polymerization-induced phase separation in a liquid-crystal-polymer mixture has been demonstrated by using light scattering techniques [6], the dynamics of a direct pattern writing approach by laser pulses is yet to be studied.

In this work, we demonstrate experimentally laser-induced phase separations and pattern

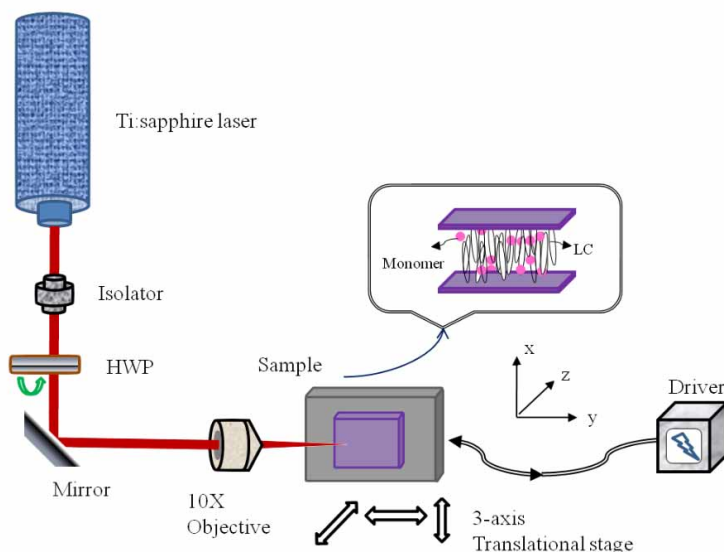


Fig. 1. Illustration of our experimental setup, where a frequency-doubled Ti:sapphire laser is focused on the sample mixed with liquid crystals (LC) and monomer molecules. A half-wave plate (HWP) is used to rotate the polarization of writing pulses. The translational stage is used to control the scanning rate of our focused beam.

formations in a liquid-crystal-monomer mixture. With adds of photo-initiators, polymerization is induced directly by a ultra-short frequency-doubled Ti:sapphire laser at the wavelength of 400nm. Different scanning rates can result in the competition among three processes, including single-photon excitation induced polymerization, phase separation morphologies, and diffusing mechanics of monomer molecules. As an example, when a femto-second laser pulse writes a straight line, a series of transition patterns for polymer structure in shapes of double-humped, single-humped and broken stripes are revealed. The mechanics underlying complex pattern formations is simulated by a modified diffusion model in $2 + 1$ dimensions, which gives a good agreement to what had been observed in experimental data. With the abilities to control phase separation morphologies and to transfer optical patterns in liquid-crystal-monomer mixtures, the laser lithography scheme studied in this work provides a promising way to fabricate complicated and sophisticate optical devices.

In the experiment, as illustrated in Fig. 1, we use a commercially tunable femto-second Ti:sapphire oscillator (Spectra-Physics Tsunami) with the wavelength at 400nm, focusing on the liquid-crystal-monomer mixtures by a 10X objective lens. The full-width-at-half-maximum (FWHM) of the focused beam, approximated by a Gaussian shape, is about $50\mu\text{m}$ in diameter. An isolator is located outside the laser cavity to prevent possible damages by back reflections, and a half-wave plate (HWP) is used to rotate the polarization of optical field. To ensure the sample is located at the focal point of laser beam, the objective is mounted on a three-axis high-resolution motorized translational stage to fine-tune its position. Our sample contains 30wt% of nematic liquid crystal *E7*, 69.4wt% monomer *NOA65* (Norland), 0.5wt% photo-initiator *Rose bengal* (Oregon medical laser center), and 0.1wt% of dye bis (2,4,6-trimethylbenzoyl) phenylphosphine oxide (Ciba: Irgacure 819). The monomer molecules have a considerable absorption peak below the wavelength at 400nm, thus the dye is added to enhance the absorption in the UV region. The mixture of liquid crystal and monomer molecules is filled into an empty cell composed by two glass substrates with a cell gap of $30\mu\text{m}$. Both of the glass surfaces

are treated with DMOAP (N, N-dimethyl-N -octadecyl-3 -aminopropyl-trimethoxysilyl chloride 6), in order to let the liquid crystal molecules stay in a homeotropically aligned state. The photo-initiators have an opened double bond, which absorbs the UV light and starts the chain reaction. Thus only at a low power of light pulse, the photo-induced polymerization process can easily extend inside the whole sample. Without adding photo-initiators, not shown here, thermo-effect plays an equivalent role as photo-induced polymerization process, resulting in a quick spreading of polymer network inside the sample. Then a uniform liquid crystal droplet distribution is formed, which scatters the light as the sample soon becomes opaque upon illuminations.

By fixing the UV light pulse duration to 300fs, the repetition rate to 80MHz, and the output power to 100mW, we perform a laser writing on the liquid-crystal-monomer sample in the shape of a straight line along one of the translation directions, labeled as the y-axis here. Before performing a detailed laser writing experiment by changing scanning speeds, first of all, we verify the pattern formation of polymer structures in the liquid-crystal-monomer mixture through the scanning electron microscope (SEM) image. After performing the photo-lithography process, we disassemble the glass substrates, wash out liquid crystal molecules by Acetones, and take SEM images for the samples by spin-coating a thin film of gold. Since liquid crystal molecules are removed, the remaining molecules shown in the SEM images can be easily identified as the formed polymer structures. Two distinct features for the formed polymer structures are shown in Fig. 2, for lower and higher scanning speeds. Figure 2(a) is a snap shot of our optical microscopic images obtained with the scanning speed at 0.1mm/sec, for which the corresponding SEM image is shown in Fig. 2(c), with a close-up picture in higher resolutions shown in Fig. 2(e). In this case, one can see a hollow-line region bounded by two polymer structures in the upper and lower sides. The difference between upper and lower sides of polymer structures in Fig. 2(e) is believed to result from the motions of monomer and polymer molecules driven by gravity due to the vertical arrangement of the samples during the writing process. Instead, at a higher scanning speed, 3mm/sec in Fig. 2(b), the formed polymer network reveals a solid line structure in the SEM image, as shown in Figs. 2(d) and (f). With the comparison between Figs. 2(a) and (c), or Figs. 2(b) and (d), one can identify that in our microscopic photos the bright region corresponds to the liquid crystal rich area, while the dark region is the polymer structure.

Later, with different scanning rates, in Figs. 3(a-d), we demonstrate a series of spontaneous optical pattern formations and phase separation morphologies recorded by an optical microscope at the speeds of 0.1, 0.5, 2, and 3mm/sec, respectively. The observed patterns are formed in the following scenario, which would be illustrated and confirmed later by our simulation results based on a modified diffusion model. It is known that the phase separation process should be dependent on the optical dose and exposure time of a writing beam. For our samples, at 20°C, the dielectric constants of liquid crystal molecules (*E7*) are $\epsilon_{\parallel} = 19.0$ and $\epsilon_{\perp} = 5.2$, respectively, while the dielectric constant of monomer molecules (*NOA65*) is 4.6 [15, 16]. Since the liquid crystal molecules have a higher dielectric constant, compared with that of monomer molecules, at a low scanning speed, as shown in Fig. 3(a), the optical field exerts a stronger force on the LC molecules than that at a high scanning speed, resulting in the formation of phase separation morphologies outside the laser writing route. The mechanics for such a phase separation morphology is similar to that reported in fringing-field-induced phase separations [8], where the gradient of electric fields imposes a force on liquid crystal molecules. Moreover, the monomer molecules are apparently pushed away to the edges, resulting in a polymerized stripe structure with a double-humped profile. The SEM images in Figs. 2(c) and (e) also provide a clear picture for such a sandwich structure. Thus, the polymerization is mainly formed along the edges of the laser lithography route, yielding an empty path of width around 200 μ m, which is wider than the focused beam size (50 μ m). In this case, the monomer molecules are driven by

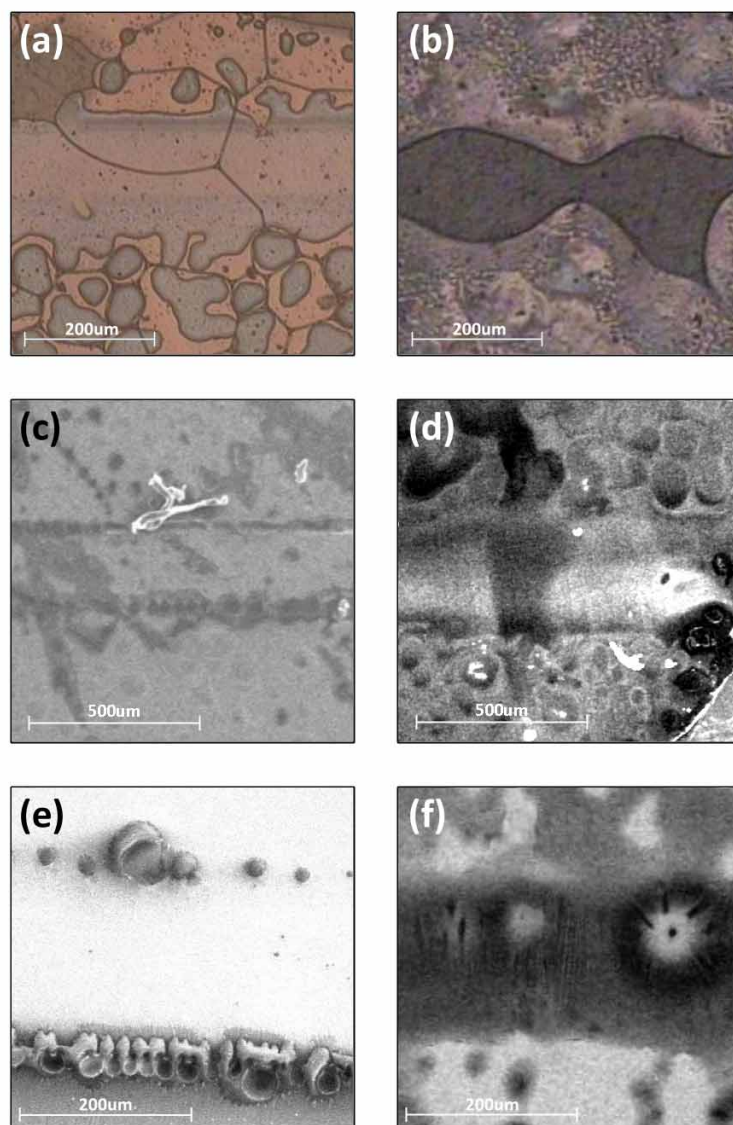


Fig. 2. Optical microscopic images of our liquid-crystal-monomer mixture, taken after the laser writing at the scanning speeds of (a) 0.1 and (b) 3mm/sec, respectively. The corresponding scanning electron microscope (SEM) images, taken after washing out the liquid crystal molecules for the samples, are shown in (c) and (d), respectively. The close-up SEM images in higher resolutions are shown in (e) and (f), respectively.

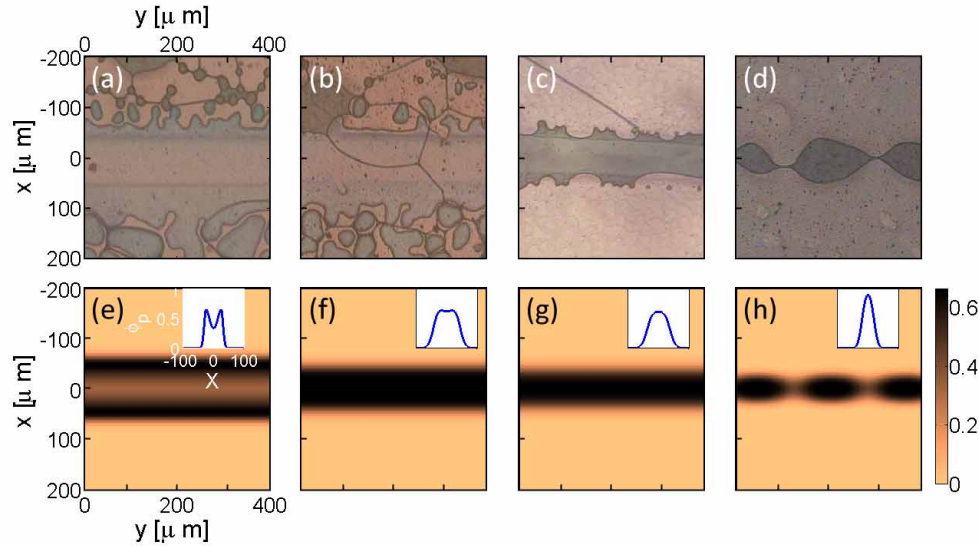


Fig. 3. Optical microscopic images of a pattern transition in photo-induced polymerization processes by a laser pulse writing at different scanning speeds of (a) 0.1, (b) 0.5, (c) 2, and (d) 3mm/sec, respectively. Dark regions represents the polymer structures, while bright region corresponds to the liquid crystal rich area. Simulation results based on a modified diffusion model for the concentration of polymer molecules are demonstrated in (e-h) for different scanning parameters: $f =$ (e) 0.001, (f) 0.01, (g) 1, and (h) 5, respectively. The insets shown in (e-h) correspond to the transverse profile of polymer molecules along the x -axis, at a fixed position $y = 0$. Other parameters used in simulations are $D_0 = 1$, $K_0 = 6$, $\alpha = 0.7$, and $A_0 = 1$.

an additional force to the edges before polymerization happens, and the repulsive force exerted on the monomer molecules comes from the writing optical field. Here, the polymer structure is formed in a double-humped profile. At this stage, the diffusion mechanism for monomer molecules is overwhelming and polymerization happens just at the edges of profile in the laser writing pulse.

When the laser scanning speed increases, as shown in Fig. 3(b) for the speed of 0.5mm/sec, the width for formed polymer structure along the laser lithography path decreases. In this case, the increase of scanning speeds makes the optical dose to be insufficient to induce polymerization. Then, the driven force from electrical field is too weak to push the monomer molecules to drift away from the edges, resulting in a narrowed but still double-humped pattern. A balance between the diffusion of molecule movement and photo-polymerization is possible to reach, resulting in the formation of a uniform polymer layer by adjusting the scanning speed. In Fig. 3(c), we report such a single polymer thin film formed at the scanning speed of 2mm/sec. Now, it can also be seen clearly that the phase separation morphologies in the surrounding regions are greatly suppressed. Moreover, at the scanning speed of 3mm/sec, as shown in Fig. 3(d), the written pattern of a straight line is transferred into a broken one due to the known symmetry-breaking instability phenomena associated with the growth of transverse modulations for quasi-one-dimensional stripes, i.e., transverse instabilities [17–19].

To explain the observed pattern transition of photon-induced polymer structures from double-humped, single-humped, to broken stripes, we use a phenomenological diffusion model and explain the kinetics of these laser-induced pattern formations. Our model is based on a modified

set of coupled diffusion equations for photo-polymers [20–22]. Let ϕ_m , ϕ_p and ϕ_{lc} be the molar concentrations of monomer, polymer, and liquid crystal, respectively. Photo-induced polymerization of the monomer molecules occurs preferentially in the area where the intensity of the laser beam is the largest. Using normalized units $x = x'/w_0$, $y = y'/w_0$ and $t = t'/(r_p I_0)$, the rate at which the concentration of monomer molecules changes can be written according to a modified Fick's law

$$\frac{\partial \phi_m}{\partial t} = \nabla [D(x, y, t) \nabla \phi_m(x, y, t)] - F(x, y, t) \phi_m(x, y, t), \quad (1)$$

where $D(x, y, t) = D_0 \exp[-\alpha \phi_p(x, y, t)]$ is the diffusion coefficient, which is also a function of space (x, y) and time (t) as the growing polymer network will affect the behavior of monomer diffusion. In this diffusion coefficient, according to the literature [23], we assume that the decay constant α depends on the weight of monomer molecules, while the constant $D_0 = d_0/(r_p I_0 w_0^2)$ associated with the diffusion coefficient of monomers d_0 (ranges from 10^{-10} - $10^{-11} \text{ cm}^2 \text{ s}^{-1}$), the polymerization rate r_p (ranging from 70 - $1000 \text{ Lmol}^{-1} \text{ s}^{-1}$), the intensity of the laser beam I_0 (100 mWcm^{-1}), and the width of the beam w_0 . The polymerization rate is described by the function $F(x, y, t)$. The negative sign implies that the monomer concentration decreases with the rate of polymerization. Polymerization is initiated in the mixture by scanning a femto-second laser along the sample, for which the reaction equation can be written as

$$\frac{\partial \phi_p}{\partial t} = F(x, y, t) \phi_m(x, y, t), \quad (2)$$

with the initial condition for polymer concentration $\phi_p(x, y, t = 0) = 0$. The local polymerization rate can be assumed in the form

$$F(x, y, t) = K_0 \exp[-\alpha \phi_p(x, y, t)] I(x, y), \quad (3)$$

with K_0 is the rate constant for polymer molecules, and $I = A_0 \exp(-x^2/w^2) \cos^2(fy)$ describes the intensity profile of our writing beam with the beam width denoted by w . The scanning speed of the laser pulse in the writing direction is described by the parameter f , which implies a higher scanning speed with a larger value. Throughout the reaction process, the total concentration of components is a constant, i.e., $\phi_{lc} + \phi_m + \phi_p = 1$. Numerical solutions are found in the steady-state, as the diffusion rate of components is required to satisfy the condition: $\frac{\partial \phi_{lc}}{\partial t} + \frac{\partial \phi_m}{\partial t} + \frac{\partial \phi_p}{\partial t} = 0$. It is known that liquid crystal molecules typically have a large diffusion coefficient, in the range 10^{-5} - $10^{-8} \text{ cm}^2 \text{ s}^{-1}$, as compared to monomers which range from 10^{-10} - $10^{-11} \text{ cm}^2 \text{ s}^{-1}$. A value of $(1.97 \pm 0.2) 10^{-8} \text{ cm}^2 \text{ s}^{-1}$ was reported for E7 in NOA65 using an *in situ* diffusion experiment [24]. This allows us to calculate the liquid crystal concentration just by the mass conservation law.

Before solving this set of diffusion equations, we want to say more about the physics inside this model. The system which we considered here is a homogeneous mixture of monomer and liquid crystal molecules. Irradiating it results in the conversion of monomer molecules to polymer network. After the laser writing process, the system is ternary consisting of monomer molecules, polymer network, and liquid crystal molecules. As the polymerization proceeds, more and more monomer molecules are converted to polymer network whereas the number of liquid crystal molecules remains invariant. The concentration profile of the liquid crystal molecules can be obtained using the mass conservation law and hence the diffusion equation for liquid-crystal molecules is not explicitly considered in the simulations. Moreover, as the reaction proceeds, the monomer molecules are converted to highly dense inter-linked polymer chains. Hence the diffusion mechanism for polymer chains can be considered negligible.

Numerical results for the polymer concentration distributions, ϕ_p , obtained by solving the set of equations in Eqs. (1)–(3) with a Crank-Nicolson finite difference scheme, are shown in Figs. 3(e–h) for different scanning speeds at the steady state. As seen from the figures, the concentration profile of the polymer is modified with the scanning speed. For a lower scanning speed, as shown in Fig. 3(e) for the scanning parameter $f = 0.001$, a clear line structure is formed with a double-humped profile demonstrated in the inset. The two major peaks for the polymer concentrations allocate outside the laser writing route, i.e., the locations at $\approx \pm 100\mu\text{m}$. Since the conversion of monomer molecules to polymer chains in the high intensity region results in a concentration gradient within the sample, this concentration gradient is a function both of the intensity of laser beam as well as the amount of exposure time. For a low scanning speed, the reaction time between the laser beam and our sample is longer. In this scenario, more and more polymerized monomer molecules are pushed away from the center region, which gives the reason to form a double-humped profile in the polymer chains. This phenomenon is not only revealed in our 2D simulation results, but also verified by our experimental data both in optical microscopic and SEM images shown in Figs. 3(a) and 2(c), respectively.

As the writing speed increases, this double-humped profile is transformed into a single-humped one, as shown in Figs. 3(f) and (g), for the scanning parameters $f = 0.01$ and 1 , respectively. Now, the optical dose received by the sample is less and the polymerization takes place in the center region, resulting in the formation of a straight line with a single-humped profile. If we further increase the scanning speed, such a straight line of polymer chains suffers the modulation along the writing direction, i.e., y -axis. A broken line in the polymer concentration is demonstrated in our simulations, as shown in Fig. 3(h) with the scanning parameter $f = 5$, which gives a good agreement to what observed in our optical microscopic image shown in Fig. 3(d), as well as the SEM images shown in Fig. 2(d). Such a transverse (or symmetry-breaking) instabilities of stripe lines have been reported experimentally for different types of nonlinear systems [25]. By considering the liquid crystal-monomer mixture and photo-induced polymerization, our experimental observations differ considerably from earlier studies.

Before conclusion, we give a simple illustration on the different combinations of these four parameters, i.e., D_0 , K_0 , α , and A_0 , used in our numerical simulations. By dimensional analysis, one can introduce a dimensionless *kinetic parameter* K_p , defined as $K_p = D_0 f^2 / (K_0 A_0)$. The variation of this kinetic parameter, brought about by varying any of the constants, will result in different concentration profiles. In fact, this is manifested in the observed 2D profiles in Fig. 3(e–h) where even though D_0 , K_0 and A_0 are constants, the parameter f is varied resulting in different K_p and hence different concentration profiles. For a small value of K_p , the concentration profile will have a double-hump profile. But with increasing K_p value, the concentration profile will increasingly become similar to the profile of the input beam.

To conclude, manipulation of phase separation morphologies and pattern formation for a liquid-crystal-monomer mixture is carried out with an ultra-short UV light source. By writing at different scanning speeds with a femto-second laser pulse along a line, we experimentally demonstrate and numerically verify a series of pattern transitions for photon-induced polymer structures, with the manifestation of doubled-humped, single-humped, and broken stripes. A single polymerization strip is favored to form at a moderate scanning speed. We believe that such a laser lithography scheme provides an alternative and promising way to control phase separation morphologies and pattern transformation for liquid crystal composites.

Acknowledgments

This work is partly supported by the National Science Council of Taiwan, under the Contract numbers NSC 98-2218-E-008-004 and NSC 100-2811-M-007-044. The authors thank Yao-De Jhong for his help plotting the figures.